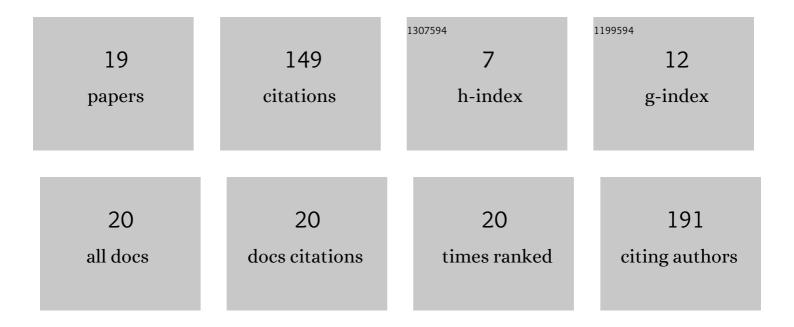
Seongmoon Jung

List of Publications by Year in descending order

Source: https://exaly.com/author-pdf/6932987/publications.pdf Version: 2024-02-01



#	Article	IF	CITATIONS
1	Europium-Diethylenetriaminepentaacetic Acid Loaded Radioluminescence Liposome Nanoplatform for Effective Radioisotope-Mediated Photodynamic Therapy. ACS Nano, 2020, 14, 13004-13015.	14.6	41
2	Evaluation of the microscopic dose enhancement for nanoparticle-enhanced Auger therapy. Physics in Medicine and Biology, 2016, 61, 7522-7535.	3.0	22
3	Dynamic <i>In Vivo</i> X-ray Fluorescence Imaging of Gold in Living Mice Exposed to Gold Nanoparticles. IEEE Transactions on Medical Imaging, 2020, 39, 526-533.	8.9	20
4	Pinhole X-ray fluorescence imaging of gadolinium and gold nanoparticles using polychromatic X-rays: a Monte Carlo study. International Journal of Nanomedicine, 2017, Volume 12, 5805-5817.	6.7	15
5	MCNP6.1 simulations for low-energy atomic relaxation: Code-to-code comparison with GATEv7.2, PENELOPE2014, and EGSnrc. Nuclear Instruments & Methods in Physics Research B, 2018, 415, 117-126.	1.4	10
6	Low-energy electron dose-point kernels and radial dose distributions around gold nanoparticles: Comparison between MCNP6.1, PENELOPE2014 and Geant4-DNA. Nuclear Instruments & Methods in Physics Research B, 2018, 430, 18-22.	1.4	8
7	Measuring radioenhancement by gold nanofilms: Comparison with analytical calculations. Physica Medica, 2019, 68, 1-9.	0.7	7
8	3D star shot analysis using MAGAT gel dosimeter for integrated imaging and radiation isocenter verification of MR‣inac system. Journal of Applied Clinical Medical Physics, 2022, 23, e13615.	1.9	7
9	Compton Background Elimination for in Vivo X-Ray Fluorescence Imaging of Gold Nanoparticles Using Convolutional Neural Network. IEEE Transactions on Nuclear Science, 2020, 67, 2311-2320.	2.0	6
10	Deriving the Effective Atomic Number with a Dual-Energy Image Set Acquired by the Big Bore CT Simulator. Journal of Radiation Protection and Research, 2020, 45, 171-177.	0.6	4
11	Dose calculation of 3D printing lead shield covered by biocompatible silicone for electron beam therapy. Physical and Engineering Sciences in Medicine, 2021, , 1.	2.4	2
12	Low Magnetic Field MRI Visibility of Rubber-Based Markers. Progress in Medical Physics, 2019, 30, 89.	0.3	1
13	Gold coated contact lens-type ocular in vivo dosimeter (CLOD) for monitoring of low dose in computed tomography: A Monte Carlo study. Physica Medica, 2021, 92, 1-7.	0.7	1
14	Monte Carlo modeling of gold nanoparticles detection limits of benchtop threeâ€dimensional L―and Kâ€shell Xâ€ray fluorescence mapping systems. X-Ray Spectrometry, 0, , .	1.4	1
15	Comparison of treatment plans between static jaw and jaw tracking techniques in postmastectomy intensity-modulated radiation therapy. Physical and Engineering Sciences in Medicine, 2022, , 1.	2.4	0
16	Assessing Commercial CLEANBOLUS Based on Silicone for Clinical Use. Progress in Medical Physics, 2021, 32, 159-164.	0.3	0
17	Effect of Total Collimation Width on Relative Electron Density, Effective Atomic Number, and Stopping Power Ratio Acquired by Dual-Layer Dual-Energy Computed Tomography. Progress in Medical Physics, 2021, 32, 165-171.	0.3	0
18	Dosimetric Characteristics of Flexible Radiochromic Film Based on LiPCDA. Progress in Medical Physics, 2021, 32, 179-184.	0.3	0

#	Article	IF	CITATIONS
19	Scanning methodology for contact lens-type ocular in vivo dosimeter (CLOD) dosimetry applying a silicone material. Radiation Oncology, 2022, 17, 88.	2.7	0